

Piezoelectric InAs/GaAs quantum dots with reduced fine-structure splitting for the generation of entangled photons

Savvas Germanis,¹ Alexios Beveratos,² George E. Dialynas,³ George Deligeorgis,⁴ Pavlos G. Savvidis,^{1,4} Zacharias Hatzopoulos,^{3,4} and Nikos T. Pelekanos^{1,4,*}

¹*Department of Materials Science and Technology, University of Crete, P.O. Box 2208, 71003 Heraklion, Greece*

²*Laboratoire de Photonique et Nanostructures LPN-CNRS, UPR-20 Route de Nozay, 91460 Marcoussis, France*

³*Department of Physics, University of Crete, P.O. Box 2208, 71003 Heraklion, Greece*

⁴*Microelectronics Research Group, IESL-FORTH, P.O. Box 1385, 71110 Heraklion, Greece*

(Received 15 September 2011; revised manuscript received 30 May 2012; published 24 July 2012)

Polarization-resolved single-dot spectroscopy reveals that the exciton fine-structure splitting in piezoelectric (211)B InAs/GaAs quantum dots is smaller than $10 \mu\text{eV}$ in the vast majority of examined dots. These values are significantly reduced compared to as-grown (100)-oriented InAs dots. Time-resolved measurements confirm the high oscillator strength of these dots, in spite of the internal piezoelectric field, suggesting good quantum efficiency at 4 K, comparable with that of (100) InAs/GaAs dots. Lastly, photon correlation measurements demonstrate single-photon emission from exciton levels of these dots. All these features make this intriguing dot system promising for implementing solid-state entangled photon sources.

DOI: [10.1103/PhysRevB.86.035323](https://doi.org/10.1103/PhysRevB.86.035323)

PACS number(s): 78.67.Hc, 78.47.jd, 77.84.—s

I. INTRODUCTION

Quantum information science strongly relies on the efficient generation of on-demand single- and entangled-photon sources.^{1,2} In several pioneering experiments,^{3–5} entangled-photon pairs were obtained using parametric down-conversion,^{6,7} which while easy to implement, suffers from the Poissonian statistics of the emitted photon pairs, leading to multipair emission, decreasing thus the fidelity of entanglement.⁸ On-demand entangled-photon pairs can be obtained by heralding a three-photon process³ or with the detection of several auxiliary photons,⁹ but both schemes are inefficient in terms of photon pair production probability. Single quantum dots (QDs) have been proposed as sources of on-demand polarization-entangled photon sources¹⁰ by using the radiative decay of two electron-hole pairs trapped in the QD. The subsequent decay of the biexciton (XX) and exciton (X) states will produce polarization-entangled photon pairs as long as the two possible decay paths to the ground state, $|\sigma^+_{XX}\rangle|\sigma^-_X\rangle$ and $|\sigma^-_{XX}\rangle|\sigma^+_X\rangle$, are indistinguishable. In actual QDs, due to lateral anisotropies of the dot wave functions, a fine-structure splitting (FSS) of the intermediate X level arises, rendering the two paths distinguishable and diminishing the entangled photon pair fidelity.^{11,12} Several techniques, using QD annealing,¹³ in-plane magnetic¹⁴ or electric field,¹⁵ perpendicular electric field,^{16,17} and biaxial strain,¹⁸ have been suggested to reduce or cancel FSS. Moreover, broadening of the X line by the Purcell effect has been used to make the two paths indistinguishable.¹² Generation of polarization-entangled photons has been reported in the last few years by using one or several of the above techniques.^{19–21} While these techniques are successful, they are hardly scalable, as it is not simple to obtain a QD with FSS below $2 \mu\text{eV}$, necessary for the generation of high-fidelity entangled photons.¹²

Alternatively, it has been proposed recently that QDs grown along polar orientations, such as (111) or (211), are capable of negligible FSS values^{22,23} based on the following considerations. Unlike the (100) dots, where lateral piezoelectric (PZ) fields elongate the electron and hole wave functions in the

growth plane generating thus significant FSS,²³ in the case of (111) or (211) dots, the main manifestation of the PZ effect is a strong vertical PZ field ($\geq 1 \text{ MV/cm}$),^{24–26} which does not introduce any lateral wave function anisotropy, and hence does not generate FSS. Lateral PZ fields are also present in these orientations; however, they are much weaker and, as shown for (111) dots, they do not generate FSS either, as they preserve the C_{3v} symmetry of the confining potential. We argue that this equally applies to our (211) dots, not only because a (211) surface closely resembles the (111) surface but, in addition, due to the large diameter-to-height aspect ratio in our dots (≥ 10), minimizing any influence that lateral facets may have in the system. A recent work on (111) InGaAs/GaAs QDs fabricated using droplet epitaxy has indeed shown evidence for reduced FSS values ($10\text{--}40 \mu\text{eV}$),²⁷ although clearly such values are still too large for entanglement applications. On the other hand, another recent report on pyramidal InGaAs QDs grown by metal-organic chemical vapor deposition on prepatterned (111)B GaAs substrates²⁸ has reported very small FSS splittings ($< 5 \mu\text{eV}$, in the majority of dots) as well as evidence for polarization entanglement out of these higher symmetry dots. In this paper, we present results on InAs/GaAs QDs grown along the (211)B orientation in the standard Stranski–Krastanow growth mode, which as grown exhibit FSS values smaller than $10 \mu\text{eV}$, for over 90% of the dots, suggesting that (211)B-grown QDs may prove suitable for use in entangled photon sources, without necessitating any pre patterning or postprocessing step.

II. EXPERIMENTAL DETAILS

The sample used in this study was grown by molecular beam epitaxy on a (211)B semi-insulating GaAs substrate. It contains a single layer of InAs QDs, grown in the middle of a 10-nm-thick GaAs/Al_{0.3}Ga_{0.7}As quantum well, about 50 nm beneath the sample surface. The QD layer is grown by depositing 1.5 monolayers (MLs) of InAs at 500 °C with a growth rate of 0.1 ML/s. Under these growth conditions, the InAs dots take the shape of truncated pyramids, with typical

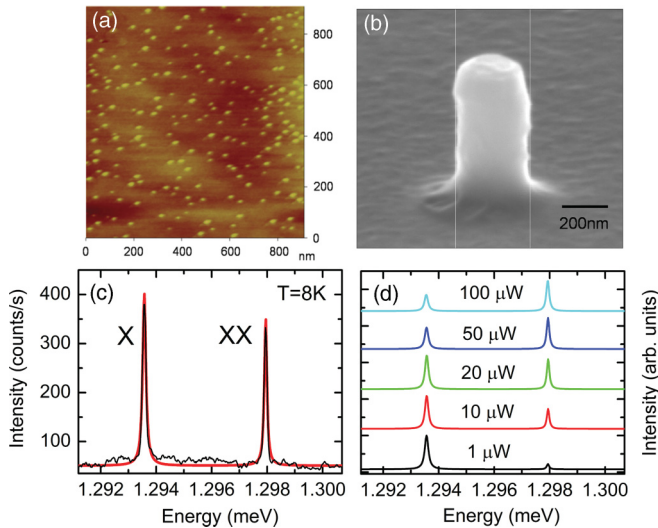


FIG. 1. (Color online) (a) AFM image from an uncapped QD layer grown at the same conditions as in the sample used in this work. (b) SEM picture from a typical mesa used for μ -PL experiments. (c) μ -PL spectrum from a single (211)B InAs/GaAs QD consisting of an excitonic (X) and a bi-excitonic (XX) peak. Lorentzian fittings of the two peaks are superposed. The intensity axis is given in counts per second. (d) Power-dependent μ -PL spectra from the same QD, manifesting the strongly nonlinear character of the XX line. The spectra are upshifted for clarity and normalized to the maximum peak.

QD heights between 2 and 3 nm, an aspect ratio larger than 10, and a QD density of $\sim 10^{10} \text{ cm}^{-2}$.²⁹ As an example, Fig. 1(a) presents an atomic force microscopy (AFM) image from an uncapped QD sample grown at exactly the same conditions, the analysis of which reproduces the above values well. For single-dot spectroscopy, the sample is processed by e-beam lithography into mesas of various diameters (150–500 nm), placed more than $15 \mu\text{m}$ apart. A typical mesa is shown in Fig. 1(b). A continuous-wave 405-nm laser diode is used for the excitation of isolated mesas with a spot size of $\sim 5 \mu\text{m}$. The micro-photoluminescence (μ -PL) signal is dispersed in a 0.75-m spectrograph with 1200-gr/mm grating and is detected by a Nitrogen-cooled charge-coupled device camera. Taking into account the instrument's spectral resolution and typical line widths of $100 \mu\text{eV}$, the resolving power of this setup using standard deconvolution procedure is estimated to be $\sim 10 \mu\text{eV}$. One can further improve the precision of the FSS measurement beyond this $10 \mu\text{eV}$ limit by applying the method of Ref. 13, i.e. utilizing Lorentzian fittings to determine the energies of the exciton (X) and biexciton (XX) peaks, and subsequently fitting the XX-X energy difference vs polarization angle by a sinusoidal function where applicable. The sample is cooled down to 5 K in a variable-temperature continuous-flow helium cryostat. The polarization-resolved spectra are recorded using a fixed linear polarizer in front of the spectrograph and a broadband $\lambda/2$ wave plate to rotate the polarization. For the time-resolved PL experiments, a mode-locked Ti:sapphire laser at 780 nm was used with 4 ps pulses at 81 MHz repetition rate.

III. RESULTS AND DISCUSSION

A characteristic μ -PL spectrum from a single (211)B InAs/GaAs QD is presented in Fig. 1(c). It consists of two

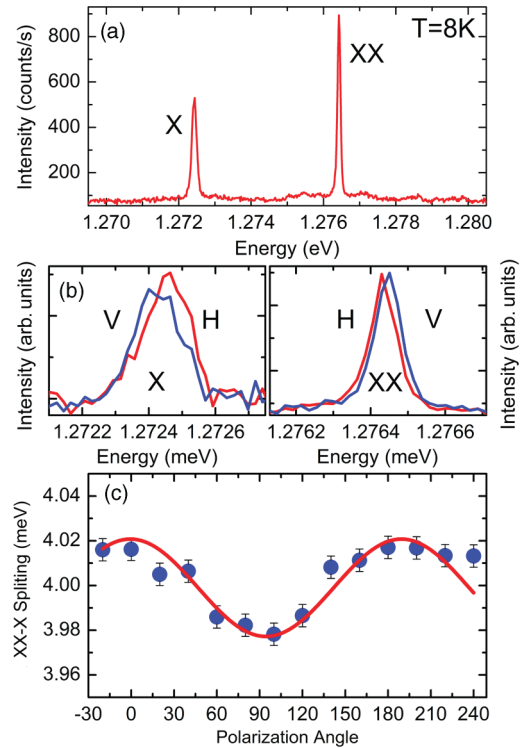


FIG. 2. (Color online) (a) μ -PL spectrum from a (211)B InAs/GaAs QD with sizable FSS, consisting of the characteristic exciton (X) and bi-exciton (XX) peaks. (b) Polarization-resolved emission from the X and XX lines of same dot. (c) XX-X energy splitting as a function of polarization angle, showing characteristic periodicity. The extracted FSS for this QD is $20 \mu\text{eV}$.

lines, labeled as X and XX, which have been identified as exciton and bi-exciton emission peaks, based on their linear and quadratic power dependence, respectively, at low excitation powers. The related power-dependent spectra, demonstrating the strongly nonlinear character of the XX line, are depicted in Fig. 1(d). In fact, the intensity of X scales as $\sim P^{0.89}$ at low powers, whereas that of XX as $\sim P^{1.8}$. The energy difference between the XX and X lines is $\sim 4.4 \text{ meV}$ in this QD, with the XX line appearing characteristically at higher energy as a manifestation of the huge PZ field inside the dots, determined to be $\sim 1 \text{ MV/cm}$ based on our own measurements.^{25,26} Alternative assignments for the two lines involving charged excitons can be easily ruled out, based on the observed power dependence and the fact that, in undoped QD systems as ours, charged excitons are typically observed as additional lines to the neutral exciton ones. For instance, the possibility to interpret the XX line as due to a charged exciton can be excluded, not only based on its near quadratic power dependence, but also on the fact that, in such a case, a third distinct bi-excitonic line would be expected at the exciton saturation excitation levels, which is not observed in our dots. Moreover, for the particular dot discussed in Fig. 2, showing a sizable FSS ($> 10 \mu\text{eV}$), if either or both of the lines were due to charged excitons, they should not exhibit any linear polarization splitting,³⁰ unlike the experimental findings of Fig. 2.

To determine FSS in (211)B InAs/GaAs QDs, we performed polarization-dependent μ -PL on 20 different single

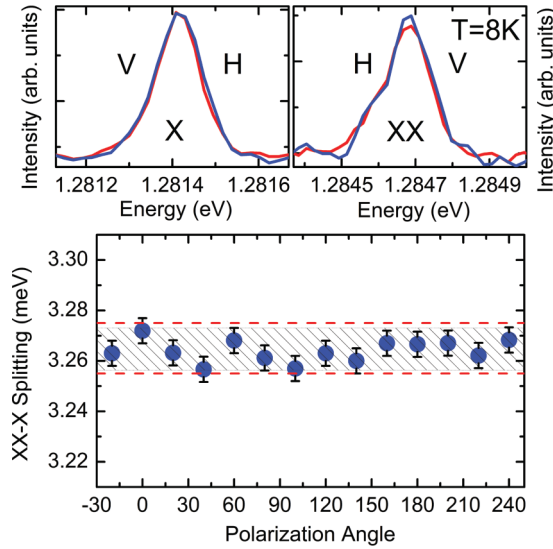


FIG. 3. (Color online) Top: Polarization-resolved emission from the X and XX lines of a typical (211)B InAs/GaAs QD, exhibiting very weak polarization dependence. Bottom: XX-X energy splitting as a function of polarization angle, showing no obvious periodicity. All points lie within the 20- μ eV-wide shaded zone, implying that the FSS is less than 10 μ eV.

dots of the sample. Among these, only two have shown FSS larger than our resolving power of 10 μ eV. One such case is shown in Fig. 2, where the X and XX emission lines of Fig. 2(a) are analyzed in terms of linear polarization in Fig. 2(b). We observe that, while the intensity of the lines remains practically intact, their energy positions vary periodically with polarizer angle, shifting in opposite directions. By extracting the energy positions by Lorentzian fittings, the XX-X energy difference is plotted in Fig. 2(c) as a function of polarizer angle, exhibiting the characteristic sinusoidal periodicity of 180°. From the max-min energy difference, we deduce that the FSS in this QD is 20 μ eV. However, as previously mentioned, 90% of the dots tested in this work have shown FSS below 10 μ eV. A typical example is depicted on the top panel of Fig. 3, where the X and XX lines of another dot appear nearly completely insensitive to polarization. The extracted XX-X energy difference is plotted as a function of polarizer angle on the bottom panel of Fig. 3, showing no obvious sinusoidal behavior. However, all data points lie within the 20 μ eV shaded zone, clearly suggesting that the FSS of this dot is smaller than 10 μ eV. Similar behavior has been observed for 90% of the examined dots. In order to assign an FSS value to all our dots, we subtract the XX-X energy difference values at 0° and 90° polarization angle and divide by two. The thus-obtained FSS values are plotted in the histogram of Fig. 4, confirming that only 10% of the QDs exhibit a splitting larger than 10 μ eV. By assuming a Gaussian distribution, we obtain a mean FSS of 6.2 ± 3 μ eV. This is to be compared to FSS values of several tens of μ eV for as-grown (100) InAs/GaAs QDs,¹³ which can be reduced to less than 10 μ eV only when annealing is applied to specific dots.³¹

Negligible FSS is not a sufficient condition to make the (211)B InAs/GaAs QDs a good candidate for the generation of entangled photon pairs. It is necessary that these QDs

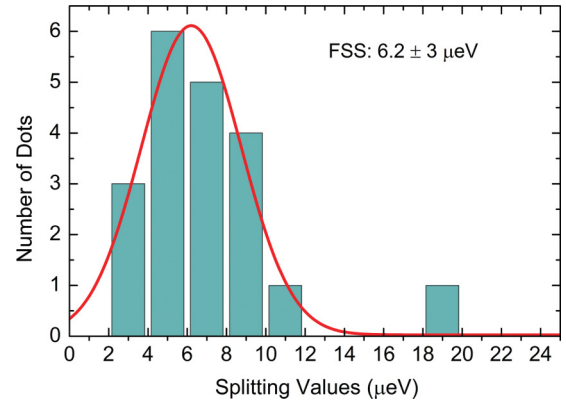


FIG. 4. (Color online) Statistical distribution of the FSS values fitted with a Gaussian along with mean and full width half maximum values.

exhibit purely radiative decay and single-photon emission. We investigated both properties under pulsed excitation in a time-resolved μ -PL setup. Figure 5(a) depicts the PL decay curves obtained at 5 K from the X line of a single dot emitting at 1.2778 eV for two different excitation powers. By fitting the decay curves at long times with a single exponential, we extract a lifetime of ≈ 2 ns, independent of the pump power, as

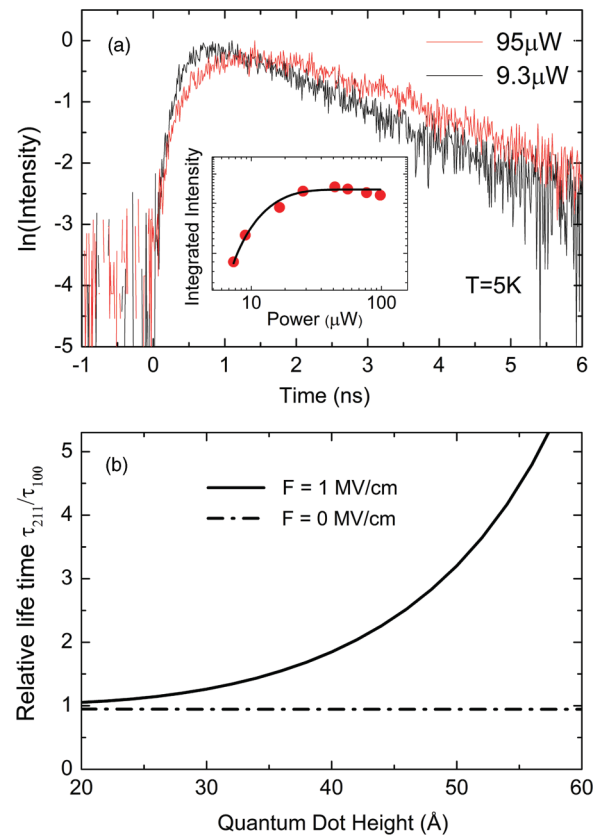


FIG. 5. (Color online) (a) Time-decay curves of the X line of a single (211)B InAs QD as a function of excitation power. The inset shows the time-integrated PL intensity vs power, marking a clear saturation regime in this power range. (b) Calculated ratio of radiative lifetimes in (211) and (100) QDs as a function of QD height, with or without a PZ field of 1 MV/cm in the (211) dots.

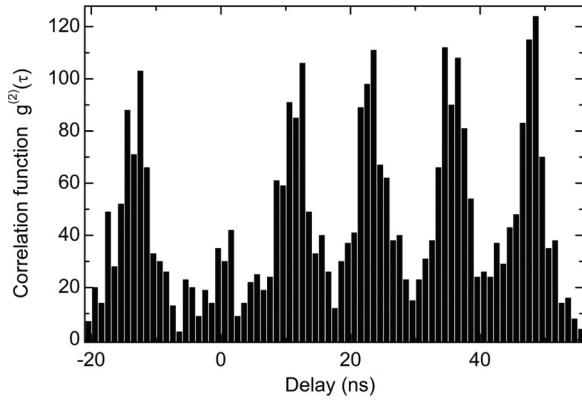


FIG. 6. Second-order correlation function $g^2(\tau)$ obtained with $27 \mu\text{W}$ pump power demonstrating clear antibunching behavior characteristic of single photon emission.

expected for QD emission. This lifetime is comparable to the ones observed in (100) InAs/GaAs QDs emitting in the same energy range.^{32–34} Specifically, Karachinsky *et al.*³² reported a 2-ns lifetime for InAs dots emitting at 1.30 eV; Bardot *et al.*³³ 1.55 ns for dots emitting at 1.29 eV; and Ulrich *et al.*³⁴ 1 ns at 1.34 eV. This demonstrates the still high oscillator strength and quantum efficiency of the (211) dots in spite of the large PZ field of $\sim 1 \text{ MV/cm}$, which is expected to reduce the oscillator strength and increase the radiative lifetime by quantum-confined Stark effect (QCSE). In order to understand this important point, we plot in Fig. 5(b) the calculated ratios of radiative lifetimes in (211) and (100) QDs as a function of QD height, with or without a PZ field of 1 MV/cm in the (211) dots, assuming a one-dimensional (1D) Schrödinger equation model and calculating the electron-hole wave function overlap integrals in the envelope function approximation. Strain effects on the band alignment and the effective mass dependence on growth direction have been taken into account. The 1D simplification is justified in our case by the large aspect ratio of the QDs (> 10), implying that quantum confinement along the growth direction is much stronger compared to the lateral directions. For zero field, the lifetime ratio is practically constant and close to unity, while for the 1 MV/cm PZ field, the ratio increasingly deviates from unity with increasing QD height, in accordance to QCSE. However, for QD heights between 2–3 nm, which are the actual heights of our dots, the lifetime ratio barely exceeds unity by only 10–30%, accounting for the relatively short lifetimes observed in our experiments. Coming back to Fig. 5(a), the prolonged rise-time observed in the PL

decay curve for $95 \mu\text{W}$ is attributed to state filling and subsequent cascade from higher excited dot levels.³⁵ The same state-filling effects are responsible for the strong saturation of the PL intensity, depicted in the inset of Fig. 5(a). Note that both the 2-ns lifetime and the observation of state filling constitute an indirect proof of the high optical quality of the (211) InAs/GaAs QDs, equivalent to their well-known (100) counterparts.

Finally, single-photon emission is direct proof of the single-exciton nature of the investigated QD. The experiment was performed in a typical Hanbury–Brown–Twiss setup with two avalanche photodiodes (APD EG&G Model SPCM-AQR 13).³⁶ Each APD is placed after a monochromator, spectrally filtering the X line, to avoid optical crosstalk.³⁷ The same single dot of Fig. 5(a) is pumped with a power of $27 \mu\text{W}$, i.e. just below saturation, in order to maximize the photon count rate. The count rates were 6500 and 9000 counts per second (cps) on each APD with a background of 2500 and 4000 cps, respectively, measured next to the X line. The background arises from emission in a doped buffer layer of the sample, but also from stray light on the APDs (≈ 1000 cps). Figure 6 shows the raw second-order autocorrelation function $g^2(\tau)$ of the X line, after integration of 3600 s. At each repetition of the laser pulse, we observe a correlation peak, the area under which normalizes to $A(\tau) = 1 \pm 0.05$.³⁶ At $\tau = 0$, however, we observe absence of coincidences, signature of single-photon emission from the dot under investigation. The normalized area of the $\tau = 0$ peak is $A(\tau = 0) = 0.28 \pm 0.05$, which is less than 0.5, satisfying the criterion for single-photon emission. Note that the $g^2(\tau)$ function has not been corrected for any background, and the relatively poor value of $A(\tau = 0)$ is mostly due to the excess of background noise.

IV. CONCLUSION

In conclusion, we have shown that (211) InAs/GaAs QDs are good candidates for the implementation of compact entangled-photon sources. We have demonstrated that the mean FSS splitting of these dots as grown is below $10 \mu\text{eV}$. In addition, we have shown that their lifetimes are very similar to their (100) counterparts and that they are capable of single-photon emission.

ACKNOWLEDGMENTS

This work was cofunded by the European Social Fund and National Resources through the program HERAKLEITUS II, and the C’NANO “Au fil de l’eau” program.

*Corresponding author: pelekano@physics.uoc.gr

¹P. W. Shor, *SIAM J. Comput.* **26**, 1484 (1997).

²L. K. Grover, *Phys. Rev. Lett.* **79**, 325 (1997).

³J. W. Pan, D. Bouwmeester, H. Weinfurter, and A. Zeilinger, *Phys. Rev. Lett.* **80**, 3891 (1998).

⁴R. Prevedel, P. Walther, F. Tiefenbacher, P. Böhi, R. Kaltenbaek, T. Jennewein, and A. Zeilinger, *Nature* **445**, 65 (2007).

⁵M. Halder, A. Beveratos, N. Gisin, V. Scarani, C. Simon, and H. Zbinden, *Nature Phys.* **3**, 692 (2007).

⁶Z. Y. Ou and L. Mandel, *Phys. Rev. Lett.* **61**, 54 (1988).

⁷P. G. Kwiat, K. Mattle, H. Weinfurter, A. Zeilinger, A. V. Sergienko, and Y. Shih, *Phys. Rev. Lett.* **75**, 4337 (1995).

⁸V. Scarani, H. de Riedmatten, I. Marcicic, H. Zbinden, and N. Gisin, *Eur. Phys. J. D* **32**, 129 (2005).

⁹S. Barz, G. Cronenberg, A. Zeilinger, and P. Walther, *Nat. Photon.* **4**, 553 (2010).

¹⁰O. Benson, C. Santori, M. Pelton, and Y. Yamamoto, *Phys. Rev. Lett.* **84**, 2513 (2000).

- ¹¹T. M. Stace, G. J. Milburn, and C. H. W. Barnes, *Phys. Rev. B* **67**, 085317 (2003).
- ¹²M. Larqué, I. Robert-Philip, and A. Beveratos, *Phys. Rev. A* **77**, 042118 (2008).
- ¹³R. J. Young, R. M. Stevenson, A. J. Shields, P. Atkinson, K. Cooper, D. A. Ritchie, K. M. Groom, A. I. Tartakovskii, and M. S. Skolnick, *Phys. Rev. B* **72**, 113305 (2005).
- ¹⁴M. Bayer, G. Ortner, O. Stern, A. Kuther, A. A. Gorbunov, A. Forchel, P. Hawrylak, S. Fafard, K. Hinzer, T. L. Reinecke, S. N. Walck, J. P. Reithmaier, F. Klopff, and F. Schäfer, *Phys. Rev. B* **65**, 195315 (2002).
- ¹⁵K. Kowalik, O. Krebs, A. Lemaître, S. Laurent, P. Senellart, P. Voisin, and J. A. Gaj, *Appl. Phys. Lett.* **86**, 041907 (2005).
- ¹⁶A. J. Bennett, M. A. Pooley, R. M. Stevenson, M. B. Ward, R. B. Patel, A. Boyer de la Giroday, N. Sköld, I. Farrer, C. A. Nicoll, D. A. Ritchie, and A. J. Shields, *Nat. Phys.* **6**, 947 (2010).
- ¹⁷J. D. Plumhof, V. Křápek, F. Ding, K. D. Jöns, R. Hafenbrak, P. Klenovský, A. Herklotz, K. Dörr, P. Michler, A. Rastelli, and O. G. Schmidt, *Phys. Rev. B* **83**, 121302(R) (2011).
- ¹⁸M. Ghali, K. Ohtani, Y. Ohno, and H. Ohno, *Nature Communications* **3**, 661 (2012).
- ¹⁹A. Dousse, J. Suffczyński, A. Beveratos, O. Krebs, A. Lemaître, I. Sagnes, J. Bloch, P. Voisin, and P. Senellart, *Nature* **466**, 217 (2010).
- ²⁰R. M. Stevenson, R. J. Young, P. Atkinson, K. Cooper, D. A. Ritchie, and A. J. Shields, *Nature* **439**, 179 (2006).
- ²¹N. Akopian, N. H. Lindner, E. Poem, Y. Berlatzky, J. Avron, D. Gershoni, B. D. Gerardot, and P. M. Petroff, *Phys. Rev. Lett.* **96**, 130501 (2006).
- ²²R. Singh and G. Bester, *Phys. Rev. Lett.* **103**, 063601 (2009).
- ²³A. Schliwa, M. Winkelnkemper, A. Lochmann, E. Stock, and D. Bimberg, *Phys. Rev. B* **80**, 161307 (2009).
- ²⁴G. Bester, X. Wu, D. Vanderbilt, and A. Zunger, *Phys. Rev. Lett.* **96**, 187602 (2006).
- ²⁵G. E. Dialynas, S. Kalliakos, S. I. Tsintzos, Z. Hatzopoulos, and N. T. Pelekanos (unpublished).
- ²⁶G. E. Dialynas, N. Hadjidimitriou, S. Kalliakos, S. Tsintzos, P. G. Savvidis, Z. Hatzopoulos, and N. T. Pelekanos, *Phys. Status Solidi A* **205**, 2566 (2008).
- ²⁷E. Stock, T. Warming, I. Ostapenko, S. Rodt, A. Schliwa, J. A. Töfflinger, A. Lochmann, A. I. Toropov, S. A. Moshchenko, D. V. Dmitriev, V. A. Haisler, and D. Bimberg, *Appl. Phys. Lett.* **96**, 093112 (2010).
- ²⁸A. Mohan, M. Felici, P. Gallo, B. Dwir, A. Rudra, J. Faist, and E. Kapon, *Nature Photonics* **4**, 302 (2010).
- ²⁹G. E. Dialynas, S. Kalliakos, C. Xenogianni, M. Androulidaki, T. Kehagias, P. Komninou, P. G. Savvidis, Z. Hatzopoulos, and N. T. Pelekanos, *J. Appl. Phys.* **108**, 103525 (2010).
- ³⁰G. A. Narvaez, G. Bester, and A. Zunger, *Phys. Rev. B* **72**, 245318 (2005).
- ³¹D. J. P. Ellis, R. M. Stevenson, R. J. Young, A. J. Shields, P. Atkinson, and D. A. Ritchie, *Appl. Phys. Lett.* **90**, 011907 (2007).
- ³²L. Y. Karachinsky, S. Pellegrini, G. S. Buller, A. S. Shkolnik, N. Y. Gordeev, V. P. Evtikhiev, and V. B. Novikov, *Appl. Phys. Lett.* **84**, 7 (2004).
- ³³C. Bardot, M. Schwab, M. Bayer, S. Fafard, Z. Wasilewski, and P. Hawrylak, *Phys. Rev. B* **72**, 035314 (2005).
- ³⁴S. M. Ulrich, M. Beyoucef, P. Michler, N. Baer, P. Gartner, F. Jahnke, M. Schwab, H. Kurtze, M. Bayer, S. Fafard, Z. Wasilewski, and A. Forchel, *Phys. Rev. B* **71**, 235528 (2005).
- ³⁵C. Santori, G. S. Solomon, M. Pelton, and Y. Yamamoto, *Phys. Rev. B* **65**, 073310 (2002).
- ³⁶A. Beveratos, S. Kuhn, R. Brouri, T. Gacoin, J. P. Poizat, and P. Grangier, *Eur. Phys. J. D* **18**, 191 (2002).
- ³⁷C. Kurtsiefer, P. Zarda, S. Mayer, and H. Weinfurter, *J. Mod. Optics* **48**, 2039 (2001).